Performance of Ring-TCM Codes over Two-way Relay Fading Channels using Linear Physical-layer Network Coding

Zichao Sun †, Li Chen †, Xiaojun Yuan ‡
† School of Information Science and Technology, Sun Yat-sen University, Guangzhou, China
‡ School of Information Science and Technology, ShanghaiTech University, Shanghai, China
Emails: sunzch@mail2.sysu.edu.cn, chenli55@mail.sysu.edu.cn, yuanxj@shanghaitech.edu.cn

***Abstract*—This paper proposes a channel coded linear physical-layer network coding (LPNC) scheme for two-way relay (TWR) fading channel, where only the relay possesses the channel state information (CSI) in the multiple access (MAC) phase. This scheme employs the spectrally efficient Ring-Trellis Coded Modulation (Ring-TCM) codes to achieve a better performance for TWR communication systems that employs LPNC. The design criterion of the Ring-TCM code for TWR fading channel is discussed. We also propose a new algorithm to find the optimal network coding coefficients to resemble the channel fading coefficients of the node-to-relay channels. The relay estimates the end nodes' message using the maximum *a posteriori* (MAP) decoding algorithm based on a joint trellis. Our simulation results show that the coded LPNC scheme significantly outperforms the uncoded LPNC scheme. It can also outperform the coded scheme that employs complete decoding (CD) scheme. Our simulation results also show that the proposed scheme can approach the cut-set bound at the high signal-to-noise ratio (SNR).**

***Index Terms*—Channel code, linear physical network coding, two-way relay, fading channel, Ring-TCM codes.**

I. Introduction

Physical-layer network coding (PNC) [1] has the potential to dramatically increase the throughput of multi-source wireless communication networks. The two-way relay channel (TWR-C), in which two end nodes simultaneously exchange message via an intermediate relay, employs PNC at the relay and can potentially double the throughput of the conventional one-way relay channel. The essential idea of the PNC is that the relay attempts to estimate the network coding message using the superimposed symbols of the two end nodes. However, for two-way relay (TWR) communication as PNC, to deal with the amplitude variation and carrier-phase offset (CPO) of TWRC remains to be two key challenges in realistic communication scenarios.

Recently, a compute-and-forward (CF) [2] PNC strategy was studied in [3–5], which is referred as linear PNC (LPNC). LPNC performs linear combination of the end nodes message using ring operation, while the convolutional PNC combines the end nodes' message (in bits) using the exclusive-or (XOR) operation. The LPNC can well address the amplitude variation and CPO problems and minimize the error probability of the network coding message by choosing the optimal integer coefficients to resemble the channel fading coefficients experienced by the transmitted symbols of the end nodes. Compared with PNC, LPNC has multiple network coding combinations, so it can significantly reduce the influence from the amplitude variation and CPO by choosing the optimal integer coefficients for network coding message. They can be seen as the optimal network coding coefficients which can minimize the error probability of the network coded message. A real-valued system model with LPNC was studied in [3]. Both real and complex-valued system models with LPNC were studied in [4, 5]. They have proposed the design of LPNC without using a channel code. Simulation results of [4] and [5] have shown that in an uncoded system, the LPNC scheme outperforms the convolutional PNC scheme by more than 5 dB in a complex-valued Rayleigh fading TWRC. So far, LPNC has only been studied in the uncoded systems. It remains a challenge to extend LPNC to a communication system that employs a practical channel code.

In this paper, we investigate the design of the channel coded LPNC system for complex-valued Rayleigh fading TWRC, where only the relay possesses the channel state information (CSI) in the multiple access (MAC) phase [4]. The uncoded LPNC scheme is operated in a size-q integer set, where q is a prime number. It is necessary to utilize a channel code that is defined in the same integer set as the LPNC. However, most existing channel codes are defined in the finite field of size two or its extension field, except the Ring-Trellis Coded Modulation (Ring-TCM) codes [6–8] and the lattice codes [9, 10]. In practice, lattice codes are difficult to implement due to its high encoding and decoding complexity, leaving Ring-TCM codes as a suitable channel code to be employed. The other advantage of Ring-TCM code is its capability in achieving high spectrum efficiency. Hence, we employ the Ring-TCM codes in the TWR communication that is assisted by LPNC. We propose a new algorithm to find the optimal network coding coefficients to resemble the channel fading coefficients for the coded system. Our simulation results show that the channel coded LPNC significantly outperforms the uncoded LPNC scheme and the the complete decoding (CD) scheme (which decodes the individual messages of end nodes). We further show that the channel coded LPNC scheme can well approach the cut-set bound of the TWRC at high signal-to-noise ratio (SNR).

The following notations are used throughout this paper. The

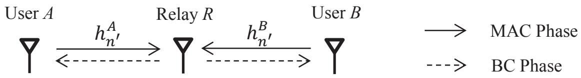

Fig. 1. Two-way relay communications using PNC.

notation Z_q denotes the ring of integers of size q and $Z_q = \{0, 1, 2, \cdots, q-1\}$. The notation $\oplus$, $\ominus$ and $\otimes$ denote the modulo-q addition, subtraction and multiplication on Z_q, as $a \oplus b \doteq \mathrm{mod}(a+b, q)$, $a \ominus b \doteq \mathrm{mod}(a-b, q)$ and $a \otimes b \doteq \mathrm{mod}(ab, q)$, where a and b are non-negative integers.

II. TWR Communications Signal Model

The TWR communication system model is shown in Fig. 1 which consists of two end nodes, A and B, and the relay node, R. There is no direct link between A and B, so they have to communicate via the R node. In this paper, the channel is assumed to be frequency-nonselective and fast fading, in which the channel state changes independent from one to another. We assume that the CSI is not known at the transmitters while it is perfectly known at the receiver.

As shown in Fig. 1, in the MAC phase, A and B simultaneously transmit their encoded message to the R node. The R node receives the superimposed symbols which are interfered by the channel. With the received signal and the CSI, the R node detects and decodes the LPNC message of A and B. In the broadcast (BC) phase, the R node re-encodes the LPNC messages and broadcasts to A and B. Then, each end node retrieve the desired message by combining the received LPNC message and its own message.

A. MAC Phase

We assume that the original message vector of end node m is denoted as $\bar{w}_m$ = [w_1^m, w_2^m, ... , w_l^m], where l is the length of the original message vector and the message is uniformly generated from Z_q $(q > 2)$, i.e.,

$$w_n^m \in \{0, 1, \cdots, q-1\}, m \in \{A, B\}, (1 \le n \le l). \quad (1)$$

For convenience, we assume both end nodes employ the same Ring-TCM encoder and the codeword vector of end node m is denoted as $\bar{c}_m$ = [c_1^m, c_2^m, ... , $c_{\frac{l}{r}}^m$], where r denotes the code rate. Two pulse amplitude modulation (PAM) signals of q levels are used to map the coded symbols $c_{2n'-1}^m$ and $c_{2n'}^m$ $(1 \le n' \le \frac{l}{2r})$ into a complex modulated symbol $x_{n'}^m = (x_{n'}^{m,\mathcal{R}}, x_{n'}^{m,\mathcal{I}})$, where $x_{n'}^{m,\mathcal{R}}$ and $x_{n'}^{m,\mathcal{I}}$ denote the real and imaginary parts of the complex modulated symbol $x_{n'}^m$, respectively. Therefore, it can be seen as a q^2-ary quadrature amplitude modulation (QAM), and presented as

$$x_{n'}^m = x_{n'}^{m,\mathcal{R}} + j x_{n'}^{m,\mathcal{I}} = \frac{1}{\gamma}[(c_{2n'-1}^m - \frac{q-1}{2}) + j(c_{2n'}^m - \frac{q-1}{2})], \quad (2)$$

where γ is the normalization factor that ensures $\mathbb{E}[|x_n^m|^2] = 1$. Let χ_m denotes the constellation diagram utilized by end node m and $x_{n'}^m \in \chi_m$. The transmitted symbol vector is denoted as $\bar{x}_m = [x_1^m, x_2^m, \cdots, x_{\frac{l}{2r}}^m]$. In the MAC phase, the signal received by the R node is

$$y_{n'} = h_{n'}^A \sqrt{E_s} x_{n'}^A + h_{n'}^B \sqrt{E_s} x_{n'}^B + z_{n'}, \quad (3)$$

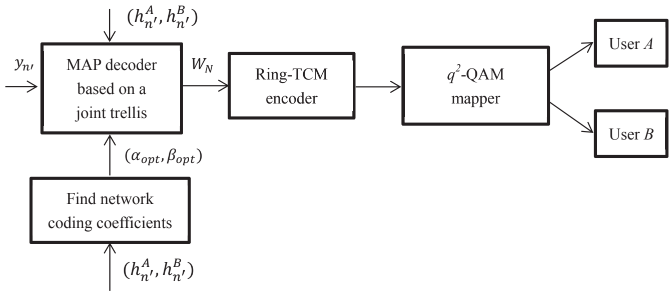

Fig. 2. Block diagram of the operation of relay.

where E_s denotes the average transmitted symbol energy and $h_{n'}^m$ denotes the complex-valued fading coefficient of the end node m-to-R channel and it is experienced by symbol $x_{n'}^m$. $z_{n'}$ is a complex-valued additive white Gaussian noise (AWGN) of zero mean and variance $\sigma^2 = N_0/2$ per dimension. The SNR is defined as $\rho \doteq E_s r/N_0$.

After the MAC transmission, the R node obtains the received signal vector $\bar{y} = [y_1, y_2, \cdots, y_{\frac{l}{2r}}] \in \mathbb{C}^{\frac{l}{2r}}$ with which it decodes the LPNC message as

$$\begin{aligned}\bar{w}_N =& \bar{\alpha} \otimes \bar{w}_A \oplus \bar{\beta} \otimes \bar{w}_B = [\alpha_1 \otimes w_1^A \oplus \beta_1 \otimes w_1^B, \\ & \alpha_2 \otimes w_2^A \oplus \beta_2 \otimes w_2^B, \cdots, \alpha_l \otimes w_l^A \oplus \beta_l \otimes w_l^B],\end{aligned} \quad (4)$$

where $\bar{\alpha}$ and $\bar{\beta}$ denote the network coding coefficient vectors as $\bar{\alpha} = [\alpha_1, \alpha_2, \cdots, \alpha_l]$ and $\bar{\beta} = [\beta_1, \beta_2, \cdots, \beta_l]$. We denote the n-th network coding message as $w_n^N = \alpha_n \otimes w_n^A \oplus \beta_n \otimes w_n^B$.

B. Operations at the R Node

Fig.2 shows the decoding and re-encoding operations at the R node. It can be described as the follows.

1) Step1: The R node finds the optimal network coding coefficients $(\alpha_{opt}, \beta_{opt})$ based on the available CSI, $h_{n'}^A$ and $h_{n'}^B$. The algorithm that finds the optimal network coding coefficients $(\alpha_{opt}, \beta_{opt})$ will be introduced in Section IV.

2) Step2: The R node decodes the end nodes' message $\bar{w}_A$ and $\bar{w}_B$ using the maximum *a posteriori* (MAP) decoding algorithm based on a joint trellis. It obtains the *a posteriori* probabilities (APP) of message symbols w_n^A and w_n^B as $P_p(w_n^A = a, w_n^B = b|\bar{y})$, where $a, b \in Z_q$. With knowledge of the optimal network coding coefficients, it can estimate the LPNC message as in (4).

3) Step3: The R node re-encodes the LPNC message and then maps the codeword to the q^2-QAM symbol for broadcasting to the end nodes.

C. BC Phase

We assume that the end nodes have knowledge of the correct network coding coefficients. With the received signal of the BC phase, two end nodes employ the MAP decoding algorithm to decode the LPNC message. In this paper, it is assumed that all nodes employ the same channel code. An end node can extract the other's message based on the decoded LPNC message, network coding coefficients and its own message. For example, node A first cancels its own message w_n^A from

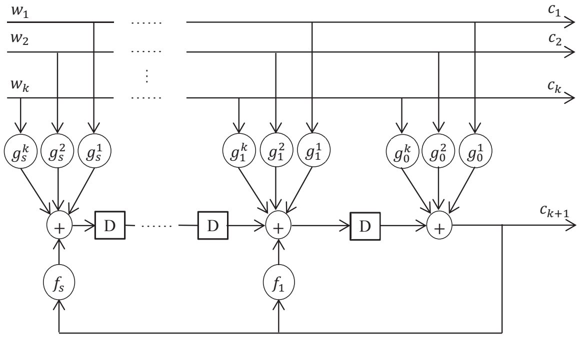

Fig. 3. Encoder structure of the Ring-TCM codes.

the decoded LPNC message. The resultant signal is multiplied with β_n^{-1}, that is the unique inverse of β_n in Z_q. The recovery process is described as

$$\beta_n^{-1} \otimes (w_n^N \ominus \alpha_n \otimes w_n^A) = \beta_n^{-1} \otimes \beta_n \otimes w_n^B = w_n^B. \quad (5)$$

In order to satisfy the condition that β_n has a unique inverse, q is required to be a prime number as in [3–5].

III. Ring-TCM Codes and MAP Decoding Based on a Joint Trellis

In our system, we employ Ring-TCM codes as the channel code for the end nodes and the MAP decoding algorithm that utilizes the joint trellis at the R node to decode the LPNC message.

A. Ring-TCM Codes

In [3–5], the LPNC is defined in Z_q. We employ the Ring-TCM codes [6–8] that is also defined in Z_q.

The encoder structure of the Ring-TCM codes is shown in Fig. 3. The encoder is represented in the form of $(g_0^1 g_0^2 \cdots g_0^k)(g_1^1 g_1^2 \cdots g_1^k) \cdots (g_s^1 g_s^2 \cdots g_s^k)/(f_1 f_2 \cdots f_s)$, where k denotes the number of input information symbols at a time and s denotes the number of the shift registers in the encoder. $g_0^1, g_0^2, \cdots, g_0^k, \cdots, g_s^1, g_s^2, \cdots, g_s^k$ are the feed-forward tap coefficients and $f_1, f_2, \cdots, f_s$ are the feedback tap coefficients. They are all defined in Z_q. The Ring-TCM code can be seen as a nonbinary TCM codes with a similar encoding process.

It has been well established in the literature that the appropriate criterion for optimal TCM design on the AWGN channel is to maximize its free Euclidean distance. However, for point-to-point fading channel, the most important parameter in designing a TCM code is the symbol Hamming weight (SHW) of the shortest error event paths [11–14]. Moreover, the trellis parallel transitions should be avoided. Since we have adopted the TWR fading channel model, the criterion for optimal Ring-TCM design in our model is still to maximize the SHW of the shortest error event paths. We will verify this criterion by our simulation results in Section V.

In this paper, we choose two Ring-TCM codes to be employed by the TWR communications that utilizes LPNC. They are Ring-TCM $(1)(1)(1)/(1,2)$ and $(2)(1)(1)/(3,2)$

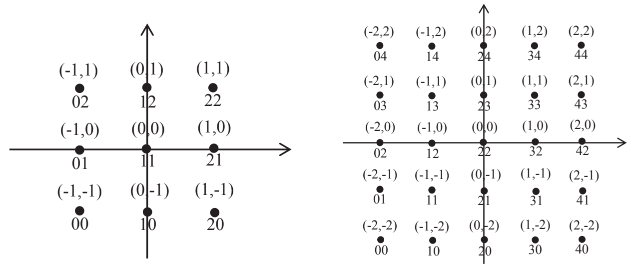

(a) Gray 9-QAM constellation (b) Gray 25-QAM constellation

Fig. 4. Gray 9-QAM and 25-QAM constellations.

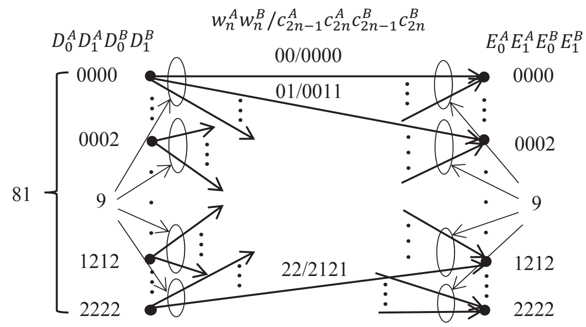

Fig. 5. Simplified joint trellis of Ring-TCM (1)(1)(1)/(1,2) code.

codes which are defined in Z_3 and Z_5, respectively. They have two shift registers and contain 9 and 25 states, respectively. The two Ring-TCM codes have the maximum SHW of the shortest error event paths constrained to the number of trellis states. And the reason that we employ systematic code is that the R node can easily calculate the network coding coefficients from the CSI which is experienced by the end nodes' original message.

It is well known that q^2-QAM Gray mapping has the optimal performance for non-iterative decoding system. So we assume that nodes A and B employ the same q^2-QAM Gray mapping. Fig. 4 shows the Gray 9-QAM and 25-QAM constellations that are integrated with the Ring-TCM $(1)(1)(1)/(1,2)$ and $(2)(1)(1)/(3,2)$ codes, respectively.

B. MAP Decoding Based on a Joint Trellis

In our system, the channel decoding is performed by the MAP decoding algorithm based on a joint trellis. That says the decoder combines the two trellis of the two end nodes to decode the LPNC message. Fig. 5 shows the simplified joint trellis structure if both of the end nodes employ the Ring-TCM $(1)(1)(1)/(1,2)$ code. Let D_i^m and E_i^m denote the current and next states of the shift register i in node m's encoder. w_n^m and c_{2n-1}^m and c_{2n}^m denote the message and codeword of the node m at time instant n, respectively. The Ring-TCM $(1)(1)(1)/(1,2)$ code is defined in Z_3 and has two shift registers. Each input message corresponds to two codeword symbols. Therefore, its joint trellis contains $3^4 = 81$ states and each state has nine incoming and outgoing branches, respectively. Note that, the R node can also decode message by MAP decoding algorithm utilizing a single trellis, but its performance is worse than that of using joint trellis and we will show this performance comparison in Section V.

With the received signal vector $\bar{y}$ and the CSI, the demapper obtains the channel observations $\Pr(y_{n'}|s_{\varrho}^{A}, s_{\varsigma}^{B})$ by

$$\Pr(y_{n'}|s_{\varrho}^{A}, s_{\varsigma}^{B}) = \frac{1}{\pi N_0} exp(-\frac{||y_{n'} - h_{n'}^{A} s_{\varrho}^{A} - h_{n'}^{B} s_{\varsigma}^{B}||^2}{N_0}), \tag{6}$$

where s_{ϱ}^{A} and s_{ς}^{B} denote the constellation points that are chosen from χ_A and χ_B, respectively, for $\varrho, \varsigma \in \{1, 2, \cdots, q^2\}$. With q^2-QAM employed at both of the end nodes, each received signal will spin out q^4 channel observations w.r.t. each distinct transmitted symbol pair $(s_{\varrho}^{A}, s_{\varsigma}^{B})$. After forward and backward traces based on the joint trellis, the MAP decoding algorithm estimates APP $P_p(\widehat{w}_n^A = a, \widehat{w}_n^B = b|\bar{y})$.

With the network coding coefficients, α_n and β_n, the MAP decoding algorithm estimates the LPNC message $\widehat{w}_N^{(\alpha_n,\beta_n)}(n)$ as in (7) and (8).

IV. LPNC for Ring-TCM Coded System

In this section, we will investigate the design of the LPNC scheme for the Ring-TCM coded TWR communication system.

For the Ring-TCM coded transmission, we know that the real and imaginary parts of the transmitted symbol $x_{n'}^{m}$ correspond to the message and parity symbols of the end node m, respectively. The LPNC message generated from the linear combination of the end nodes message can be seen as the linear combination of the real part of the symbols $x_{n'}^{A}$ and $x_{n'}^{B}$ as

$$\begin{aligned} w_n^N &= \alpha_n \otimes (\gamma x_{n'}^{A,\mathcal{R}} + \frac{q-1}{2}) \oplus \beta_n \otimes (\gamma x_{n'}^{B,\mathcal{R}} + \frac{q-1}{2}) \\ &= \alpha_n \otimes c_{2n'-1}^{A} \oplus \beta_n \otimes c_{2n'-1}^{B} \\ &= \alpha_n \otimes w_n^A \oplus \beta_n \otimes w_n^B. \end{aligned} \tag{9}$$

Note that, for $r = \frac{1}{2}$, we have $n = n'$. Therefore, the channel coded LPNC scheme is different from the uncoded LPNC [5].

The channel coded LPNC scheme consists of two steps. The first step is to calculate the network coding coefficient group. The second step is to choose the optimal network coding coefficients from the group. The two steps are described as follows.

A. Step 1: Calculating the Network Coding Coefficient Group

From [3–5], we know that the essential of the LPNC scheme is to find the optimal network coding combinations based on the CSI of TWRC. The complex superimposed symbol $\eta_{n'} = h_{n'}^{A}\sqrt{E_s}x_{n'}^{A} + h_{n'}^{B}\sqrt{E_s}x_{n'}^{B} = \eta_{n'}^{\mathcal{R}} + j\eta_{n'}^{\mathcal{I}}$ is shown as:

$$\begin{aligned} \eta_{n'}^{\mathcal{R}} &= \sqrt{E_s}(h_{n'}^{A,\mathcal{R}}x_{n'}^{A,\mathcal{R}} - h_{n'}^{A,\mathcal{I}}x_{n'}^{A,\mathcal{I}} + h_{n'}^{B,\mathcal{R}}x_{n'}^{B,\mathcal{R}} - h_{n'}^{B,\mathcal{I}}x_{n'}^{B,\mathcal{I}}), \\ \eta_{n'}^{\mathcal{I}} &= \sqrt{E_s}(h_{n'}^{A,\mathcal{I}}x_{n'}^{A,\mathcal{R}} + h_{n'}^{A,\mathcal{R}}x_{n'}^{A,\mathcal{I}} + h_{n'}^{B,\mathcal{I}}x_{n'}^{B,\mathcal{R}} + h_{n'}^{B,\mathcal{R}}x_{n'}^{B,\mathcal{I}}), \end{aligned} \tag{10}$$

where $h_{n'}^{m,\mathcal{R}}$ and $h_{n'}^{m,\mathcal{I}}$ denote the real and imaginary parts of $h_{n'}^{m}$, respectively. Clearly, there are q^4 superimposed symbols in the constellation observed by the R node.

In [5], the R node firstly calculates the minimum distance (MD) between any two superimposed symbols and calculates their symbol pair deviation based on the CSI of TWRC. The function is shown as in (11) and it obtains the symbol pair deviation $(\Delta_A^{\mathcal{R}}, \Delta_A^{\mathcal{I}}, \Delta_B^{\mathcal{R}}, \Delta_B^{\mathcal{I}})$ of the MD.

For the LPNC scheme, the optimal combination is to combine any two superimposed symbols, with symbol distance equal to MD, into the same set. The two superimposed symbols have the same LPNC message. This idea can be described by the following expression:

$$\begin{aligned} &\alpha^{\mathcal{R}} \otimes (\gamma x_{n'}^{A,\mathcal{R}} + \frac{q-1}{2}) \oplus \alpha^{\mathcal{I}} \otimes (\gamma x_{n'}^{A,\mathcal{I}} + \frac{q-1}{2}) \\ &\oplus \beta^{\mathcal{R}} \otimes (\gamma x_{n'}^{B,\mathcal{R}} + \frac{q-1}{2}) \oplus \beta^{\mathcal{I}} \otimes (\gamma x_{n'}^{B,\mathcal{I}} + \frac{q-1}{2}) \\ &= \alpha^{\mathcal{R}} \otimes c_{2n'-1}^{A} \oplus \alpha^{\mathcal{I}} \otimes c_{2n'}^{A} \oplus \beta^{\mathcal{R}} \otimes c_{2n'-1}^{B} \oplus \beta^{\mathcal{I}} \otimes c_{2n'}^{B} \\ &= \alpha^{\mathcal{R}} \otimes (c_{2n'-1}^{A} + \Delta_A^{\mathcal{R}}) \oplus \alpha^{\mathcal{I}} \otimes (c_{2n'}^{A} + \Delta_A^{\mathcal{I}}) \\ &\quad \oplus \beta^{\mathcal{R}} \otimes (c_{2n'-1}^{B} + \Delta_B^{\mathcal{R}}) \oplus \beta^{\mathcal{I}} \otimes (c_{2n'}^{B} + \Delta_B^{\mathcal{I}}), \end{aligned} \tag{12}$$

where $\alpha^{\mathcal{R}}, \alpha^{\mathcal{I}}, \beta^{\mathcal{R}}, \beta^{\mathcal{I}} \in Z_q$ are the network coding coefficients, and $(\alpha^{\mathcal{R}}, \alpha^{\mathcal{I}}, \beta^{\mathcal{R}}, \beta^{\mathcal{I}}) \neq (0, 0, 0, 0)$. Based on (12), we can imply that

$$\alpha^{\mathcal{R}} \otimes \Delta_A^{\mathcal{R}} \oplus \alpha^{\mathcal{I}} \otimes \Delta_A^{\mathcal{I}} \oplus \beta^{\mathcal{R}} \otimes \Delta_B^{\mathcal{R}} \oplus \beta^{\mathcal{I}} \otimes \Delta_B^{\mathcal{I}} = 0. \tag{13}$$

So we can find the network coding coefficient group $\mathcal{V}_c$ as

$$\mathcal{V}_c = \bigcup_{\substack{\alpha^{\mathcal{R}} \otimes \Delta_A^{\mathcal{R}} \oplus \alpha^{\mathcal{I}} \otimes \Delta_A^{\mathcal{I}} \\ \oplus \beta^{\mathcal{R}} \otimes \Delta_B^{\mathcal{R}} \oplus \beta^{\mathcal{I}} \otimes \Delta_B^{\mathcal{I}} = 0}} (\alpha^{\mathcal{R}}, \alpha^{\mathcal{I}}, \beta^{\mathcal{R}}, \beta^{\mathcal{I}}). \tag{14}$$

B. Step 2: Choosing the Optimal Network Coding Coefficients

After getting the network coding coefficient group $\mathcal{V}_c$, the R node needs to choose the optimal network coding coefficients from $\mathcal{V}_c$. We can express the real and imaginary parts of y_n' of (3) as

$$\begin{aligned} y_{n'}^{\mathcal{R}} &= \sqrt{E_s}(h_{n'}^{A,\mathcal{R}}x_{n'}^{A,\mathcal{R}} - h_{n'}^{A,\mathcal{I}}x_{n'}^{A,\mathcal{I}} \\ &\quad + h_{n'}^{B,\mathcal{R}}x_{n'}^{B,\mathcal{R}} - h_{n'}^{B,\mathcal{I}}x_{n'}^{B,\mathcal{I}}) + z_{n'}^{\mathcal{R}}, \\ y_{n'}^{\mathcal{I}} &= \sqrt{E_s}(h_{n'}^{A,\mathcal{I}}x_{n'}^{A,\mathcal{R}} + h_{n'}^{A,\mathcal{R}}x_{n'}^{A,\mathcal{I}} \\ &\quad + h_{n'}^{B,\mathcal{I}}x_{n'}^{B,\mathcal{R}} + h_{n'}^{B,\mathcal{R}}x_{n'}^{B,\mathcal{I}}) + z_{n'}^{\mathcal{I}}, \end{aligned} \tag{15}$$

where $z_{n'}^{\mathcal{R}}$ and $z_{n'}^{\mathcal{I}}$ denote the real and imaginary parts of the AWGN $z_{n'}$. Based on our earlier analysis, we only need to find the optimal LPNC combination of w_n^A and w_n^B.

In (15), the real part of the transmitted symbols $x_{n'}^{m,\mathcal{R}}$ experiences both real and imaginary parts of the CSI in $y_{n'}^{\mathcal{R}}$ and $y_{n'}^{\mathcal{I}}$. Hence, we have two methods to choose optimal coefficient based on real and imaginary parts of the CSI.

The R node calculates two MDs between any two superimposed symbols based on the real and imaginary parts of CSI, respectively. It obtains their symbol pair deviations as

$$\begin{aligned} (\Delta_{A1}^{\mathcal{R}}, \Delta_{B1}^{\mathcal{R}}) &= \arg \min_{|\delta_A^{\mathcal{R}}| + |\delta_B^{\mathcal{R}}| \neq 0} |h_{n'}^{A,\mathcal{R}}\delta_A^{\mathcal{R}} + h_{n'}^{B,\mathcal{R}}\delta_B^{\mathcal{R}}|, \\ (\Delta_{A1}^{\mathcal{I}}, \Delta_{B1}^{\mathcal{I}}) &= \arg \min_{|\delta_A^{\mathcal{I}}| + |\delta_B^{\mathcal{I}}| \neq 0} |h_{n'}^{A,\mathcal{I}}\delta_A^{\mathcal{I}} + h_{n'}^{B,\mathcal{I}}\delta_B^{\mathcal{I}}|, \end{aligned} \tag{16}$$

where $\delta_A^{\mathcal{R}}, \delta_B^{\mathcal{R}}, \delta_A^{\mathcal{I}}, \delta_B^{\mathcal{I}} \in \{1-q, \cdots, 0, \cdots, q-1\}$.

Based on the $(\Delta_{A1}^{\mathcal{R}}, \Delta_{B1}^{\mathcal{R}})$ and $(\Delta_{A1}^{\mathcal{I}}, \Delta_{B1}^{\mathcal{I}})$, the R node finds the optimal network coding coefficients from the network coding coefficient group $\mathcal{V}_c$ as

$$\widehat{w}_N^{(\alpha_n,\beta_n)}(n) = \alpha_n \otimes a^* \oplus \beta_n \otimes b^*, \tag{7}$$

where

$$\{(a^*,b^*)\} = \arg \max_{(a^*,b^*)\in\{(a,b)|\alpha_n\otimes a\oplus\beta_n\otimes b=\theta,\theta\in Z_q\}} \sum P_p(\widehat{w}_n^A = a, \widehat{w}_n^B = b|\bar{y}). \tag{8}$$

$$(\Delta_A^{\mathcal{R}}, \Delta_A^{\mathcal{I}}, \Delta_B^{\mathcal{R}}, \Delta_B^{\mathcal{I}}) = \arg \min_{\substack{|\delta_A^{\mathcal{R}}|+|\delta_A^{\mathcal{I}}|+|\delta_B^{\mathcal{R}}|+|\delta_B^{\mathcal{I}}|\neq 0,\\ \delta_A^{\mathcal{R}},\delta_A^{\mathcal{I}},\delta_B^{\mathcal{R}},\delta_B^{\mathcal{I}}\in\{1-q,\cdots,0,\cdots,q-1\}}} |(h_{n'}^{A,\mathcal{R}} + jh_{n'}^{A,\mathcal{I}})(\delta_A^{\mathcal{R}} + j\delta_A^{\mathcal{I}}) + (h_{n'}^{B,\mathcal{R}} + jh_{n'}^{B,\mathcal{I}})(\delta_B^{\mathcal{R}} + j\delta_B^{\mathcal{I}})|. \tag{11}$$

TABLE I

SYMBOL HAMMING WEIGHTS OF DIFFERENT RING-TCM CODES

Ring-TCM code	Symbol Hamming Weight (SHW)
(1)(1)(1)/(1,2)	6
(1)(1)(1)/(2,1)	5
(1)(2)(1)/(1,0)	4
(0)(2)(2)/(1,2)	3
(0)(1)(2)/(1,0)	2

$$(\alpha_{opt}, \beta_{opt}) \in \{(\alpha^{\mathcal{R}}, \beta^{\mathcal{R}})|\alpha^{\mathcal{R}}\otimes\Delta_A^{\mathcal{R}}\oplus\beta^{\mathcal{R}}\otimes\Delta_B^{\mathcal{R}}=0 \text{ or } \alpha^{\mathcal{R}}\otimes\Delta_A^{\mathcal{I}}\oplus\beta^{\mathcal{R}}\otimes\Delta_B^{\mathcal{I}}=0\}. \tag{17}$$

Note that $\alpha^{\mathcal{R}} \neq 0$ and $\beta^{\mathcal{R}} \neq 0$. If there is no $(\alpha^{\mathcal{R}}, \beta^{\mathcal{R}})$ pair satisfying the condition, the R node determines $(\alpha_{opt}, \beta_{opt}) = (1, 1)$.

Finally, the MAP decoding algorithm with a joint trellis employs the optimal network coding coefficients $(\alpha_{opt}, \beta_{opt})$ to determine the LPNC message by (7) and (8).

V. PERFORMANCE ANALYSIS AND DISCUSSION

We assume the *network coding message error* (NCME) is the event of $\widehat{w}_N^{(\alpha_n,\beta_n)}(n) \neq w_N^{(\alpha_n,\beta_n)}(n)$. In Section III, we have mentioned that the design criterion for the Ring-TCM code in TWR fading channel is to maximize the SHW of the shortest error event path. As shown in Table I, we choose five Ring-TCM codes to verify our criterion, which have different SHW of the shortest error event paths. They all have nine states in the trellis. Fig. 6 shows that the Ring-TCM $(1)(1)(1)/(1,2)$ code has the best performance as it has the greatest SHW of the shortest error event path. Meanwhile, the Ring-TCM $(1)(1)(1)/(1,2)$ code is the optimal code that we can find in the nine states trellis. The simulation result validates the proposed criterion.

Fig. 7 shows the simulation result of the Ring-TCM $(1)(1)(1)/(1,2)$ code over the TWR fading channel using LPNC and Gray 9-QAM. Our comparison benchmarks include the uncoded LPNC scheme [5], the uncoded CD scheme which completely determines all the end nodes message, coded PNC scheme which employs the MAP decoding algorithm based on a single trellis and coded CD scheme which completely determines all the end nodes' message by the MAP decoding algorithm based on a joint trellis. It can be seen that the channel-coded system significantly outperforms the uncoded

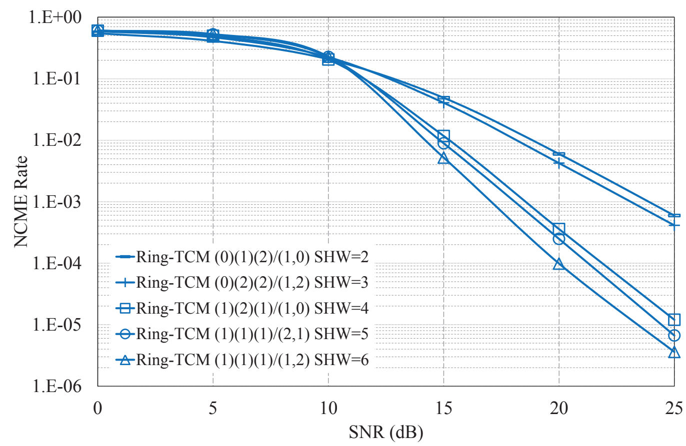

Fig. 6. NCME rate performance of 5 Ring-TCM codes LPNC scheme (9-QAM) in a fast fading TWRC.

system by more than 30 dB coding gain. For the channel-coded system, the LPNC scheme outperforms the CD scheme by $0.5 \sim 1$ dB at low-to-medium SNR. This thanks to the LPNC that performs a linear combination of the two end nodes' message. At high SNR, the LPNC scheme and the CD scheme have similar performances and approach the cut-set bound. Because the two approaches employ the APP of the symbol pairs in MAP decoding algorithm based on the joint trellis and, at high SNR, MAP decoding algorithm can correctly calculate the APP of the symbol pairs, among which one of the APP is dominant. The LPNC plays a less significant role in improving NCME.

Based on Fig. 7, we can also observe that the LPNC scheme outperforms the CD scheme by more than 5 dB in the uncoded system, while there are only $0.5 \sim 1$ dB coding gain in the channel-coded system. There are two reasons. Firstly, as mentioned above, LPNC scheme and CD scheme employ the APP of the symbol pair, which are generated from the MAP decoding algorithm. The channel coding gain has overshadowed the network coding gain. Secondly, q is not large enough for performing LPNC. For $q = 3$, there are only four possible network coding coefficients, as $(\alpha_n, \beta_n) = (1, 1), (1, 2), (2, 1)$ and $(2, 2)$. However, $(1, 1)$ and $(2, 2)$ have the same performance, and $(1, 2)$ and $(2, 1)$ have the same performance. Therefore, there are only two options

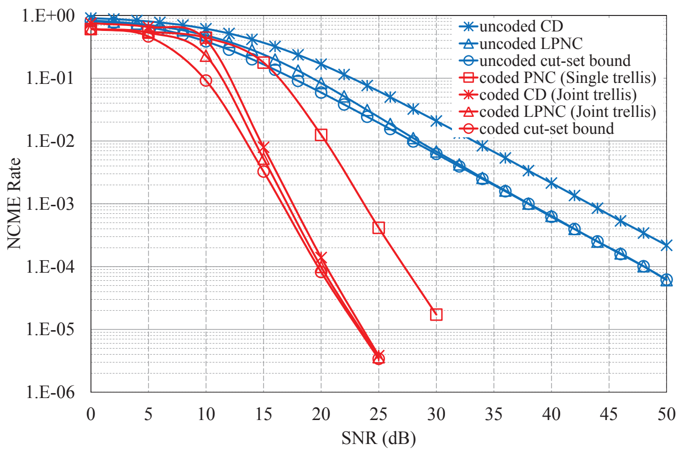

Fig. 7. NCME rate performance of Ring-TCM codes (1)(1)(1)/(1,2)(q=3) LPNC scheme (9-QAM) in a fast fading TWRC.

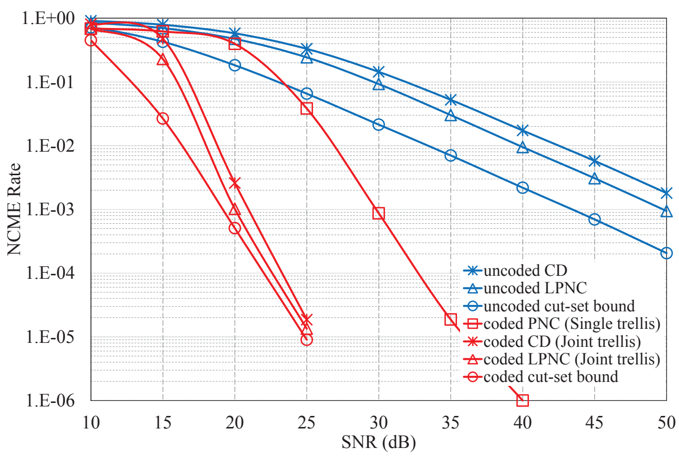

Fig. 8. NCME rate performance of Ring-TCM codes (2)(1)(1)/(3,2)(q=5) LPNC scheme (25-QAM) in a fast fading TWRC.

which cannot realize the advantages of LPNC scheme. Hence, the performance difference between LPNC scheme and CD scheme are not so significant in the channel coded system.

Fig. 8 shows the simulation result of the Ring-TCM $(2)(1)(1)/(3,2)$ coded LPNC scheme using the Gray 25-QAM. The channel code is defined in Z_5. We can see that the trend of the curve lines in Fig. 8 are similar with that of Fig. 7. The LPNC scheme outperforms the CD scheme by more than 1 dB in the channel-coded system at the low-to-medium SNR. This system model operated on Z_5 and the optional number of network coding coefficients are larger than that of Z_3. Therefore, the coded LPNC scheme can achieve a more significant coding gain over the coded CD scheme. The advantage of LPNC scheme can be realized when q is a large number.

VI. Conclusions

This paper has proposed the channel coded LPNC scheme based on Ring-TCM codes, where CSI is only available at the R node in the MAC phase. We have proposed the Ring-TCM code design criterion for TWR communication systems that employs LPNC. Using this criterion, we can find the optimal Ring-TCM code to achieve the best performance in our system model. Based on uncoded LPNC scheme and Ring-TCM codes, we have derived a new LPNC scheme to find the optimal LPNC coefficients in channel-coded system. Our simulation results have shown that the new LPNC scheme outperforms the existing schemes and can approach the cut-set bound at high SNR. We have also shown that the advantages of LPNC scheme can be realized when the system is defined in a larger integer set.

Acknowledgement

This research is supported by the National Natural Science Foundation of China (NSFC) with project ID 61372079, the National Basic Research Program of China (973 Program) with project ID 2012CB316100 and the Fundamental Research Funds for Central Universities.

References

[1] S. Zhang, S.-C. Liew, and P. Lam, “On the synchronization of physical-layer network coding,” in *Information Theory Workshop, 2006. ITW ’06 Chengdu. IEEE*, Oct 2006, pp. 404–408.
[2] B. Nazer and M. Gastpar, “Compute-and-forward: Harnessing interference through structured codes,” *IEEE Transactions on Information Theory*, vol. 57, no. 10, pp. 6463–6486, Oct 2011.
[3] T. Yang and I. Collings, “Asymptotically optimal error-rate performance of linear physical-layer network coding in rayleigh fading two-way relay channels,” *IEEE Communications Letters*, vol. 16, no. 7, pp. 1068–1071, July 2012.
[4] ——, “Design criterion of linear physical-layer network coding for fading two-way relay channels,” in *IEEE International Conference on Communications*, June 2013, pp. 3302–3306.
[5] ——, “On the optimal design and performance of linear physical-layer network coding for fading two-way relay channels,” *IEEE Transactions on Wireless Communications*, vol. 13, no. 2, pp. 956–967, February 2014.
[6] R. Baldini, A. C. F. Pessoa, and D. S. Arantes, “Systematic linear codes over a ring for encoded phase modulation,” in *Int. Symposium on Inform. and Coding Theory (ISICT 87)*, Campinas, Brazil, 1987.
[7] R. Baldini and P. Farrell, “Coded modulation based on rings of integers modulo-q. 2. convolutional codes,” *IEE Proceedings-Communications*, vol. 141, no. 3, pp. 137–142, Jun 1994.
[8] J.L.Massey and T.Mittelholzer, “Convolutional codes over rings,” in *4th. Joint Swedish-Soviet Int. Workshop on IT*, Gotland, Sweden, 1989.
[9] J. Conway and N. Sloane, “A fast encoding method for lattice codes and quantizers,” *IEEE Transactions on Information Theory*, vol. 29, no. 6, pp. 820–824, Nov 1983.
[10] ——, “Fast quantizing and decoding and algorithms for lattice quantizers and codes,” *IEEE Transactions on Information Theory*, vol. 28, no. 2, pp. 227–232, Mar 1982.
[11] M. Ahmadian-Attari and P. G. Farrell, “Efficient ring-tcm codes over fading channels,” in *Global Telecommunications Conference, 1996. GLOBECOM ’96. ’Communications: The Key to Global Prosperity*, vol. 2, Nov 1996, pp. 1248–1252.
[12] F. J. Lopez, R. A. Carrasco, and P. G. Farrell, “Ring-tcm codes for qam,” in *Satellite Communications - ECSC-3, 1993., 3rd European Conference on*, Nov 1993, pp. 341–345.
[13] R. A. Carrasco and P. G. Farrell, “Ring-tcm for fixed and fading channels: land-mobile satellite fading channels with qam,” *IEE Proceedings-Communications*, vol. 143, no. 5, pp. 281–288, Oct 1996.
[14] D. Divsalar and M. K. Simon, “The design of trellis coded mpsk for fading channels: performance criteria,” *IEEE Transactions on Communications*, vol. 36, no. 9, pp. 1004–1012, Sep 1988.